

Supporting Information

A facile and general strategy for the synthesis of porous flowerlike Pt-based nanocrystals as effective electrocatalysts for alcohols oxidation

Da-bing Huang,^a Qiang Yuan,^{*a} Pei-Lei He,^b Kai Wang^b and Xun Wang^{*b}

^a Department of Chemistry, College of Chemistry and Chemical Engineering, Guizhou University, Guiyang, Guizhou province 550025, P. R. China,

^b Department of Chemistry, Tsinghua University, Beijing 100084, P. R. China.

*E-mail: qyuan@gzu.edu.cn; wangxun@mail.tsinghua.edu.cn

Experimental section:

Chemicals: Rhodium(III) chloride hydrate (99.9%), Chloroplatinic acid hydrate (99.9%), palladium chloride (99.9%) and L-Ascorbic acid ($\geq 99.7\%$) were purchased from Sigma-Aldrich. hexadecyltrimethylammonium chloride (97%), sodium chloride (A.R.) and glycine ($\geq 98.5\%$) were purchased from China Medicine Shanghai Chemical Reagent Corp. Pt black was purchased from Johnson Matthey. Chemicals were used as received without further purification. The super pure water (18 M Ω cm) was used as solvent.

Synthesis of flowerlike Pt, PdPt, RhPt and RhPdPt nanocrystals

In a typical synthesis flowerlike nanocrystals: 0.044 g L-Ascorbic acid, 0.128 g hexadecyltrimethylammonium chloride and 0.112 g glycine were added into 14.5 mL of super pure water and stirred for several minutes. Then 0.1 M Na₂PdCl₄ and 0.1 M H₂PtCl₆ aqueous solution were added by the ratio of Pd to Pt of 1:1 (0.25 mL of 0.1 M Na₂PdCl₄ and 0.25 mL of 0.1 M H₂PtCl₆ aqueous solution), after stirred several minutes, the resulting solution was transferred to a 25 mL three-necked flask, and heated up to 85 °C, maintaining at this temperature for 1.5 h before it was cooled to room temperature. The products were separated via centrifugation/washing cycles at 10000 rpm for 25 minutes for four times with ethanol/water mixture. By adjusting the ratio of Pt and Pd precursors, the other PdPt nanocrystals can be obtained.

Similarly, flowerlike Pt nanocrystals were prepared using 0.5 mL of 0.1 M H₂PtCl₆ aqueous solution as precursors. Flowerlike Rh_{3.1}Pt_{96.9} nanocrystals were prepared using 0.05 mL of 0.1 M RhCl₃ and 0.45 mL of 0.1 M H₂PtCl₆ aqueous solution as

precursors. Flowerlike $\text{Rh}_{3.4}\text{Pd}_{42.7}\text{Pt}_{63.9}$ nanocrystals were prepared using 0.05 mL of 0.1 M RhCl_3 , 0.2 mL of Na_2PdCl_4 and 0.25 mL of 0.1 M H_2PtCl_6 aqueous solution as precursors while other conditions were kept the same.

Characterizations: The X-ray diffraction (XRD) patterns of the samples were recorded on a Bruker D8 Advance diffractometer with Cu $K\alpha$ radiation ($\lambda=1.5418 \text{ \AA}$) with graphite monochromator (40 KV, 40 mA). The size and morphology of the NCs were determined by a HITACHI H-7700 transmission electron microscope (TEM) at 100 kV, and a FEI Tecnai G2 F20 S-Twin high-resolution transmission electron microscope (HRTEM) equipped with energy dispersive spectrometer (EDS) analyses at 200 kV. The high-angle annular dark-field scanning TEM (HAADF-STEM) was determined by a FEI Tecnai G2 F20 S-Twin HRTEM operating at 200 kV. The inductively coupled plasma mass spectrometry (ICP-MS) analysis of samples was performed on IRIS Intrepid II XSP (ThermoFisher).

Characterization of electrocatalytic activity:

Electrochemical experiments were carried out in a standard three-electrode cell at room temperature (25 °C) controlled by CHI 630E electrochemical analyzer (CHI Instruments, Shanghai, Chenghua Co., Ltd.). The super pure water (18 M Ω cm) purified through a Milli-Q Lab system (Nihon Millipore Ltd.) was used as solvent. The working electrode is a glassy carbon (GC, $\phi=5 \text{ mm}$) electrode embedded into a Teflon holder. Prior to the electrochemical test, the GC electrode was mechanically polished using successively alumina powder of size 1.5, 1, and 0.5 μm . It was then cleaned in an ultrasonic bath. Then took a certain amount of flowerlike nanocrystals powder and dispersed with super pure water under ultrasonic bath. The suspension of nanocrystals was spread on the GC electrode. As soon as the electrode was dried under infrared lamp, 4 μL Nafion diluents (1 wt.% Nafion® solution) was coated onto the electrode surface. A Ag/AgCl electrode and a platinum foil were used as the reference and counter electrode, respectively.

The cyclic voltammograms (CVs) were obtained in nitrogen-saturated 0.1M HClO₄ solution, and the potential was scanned from - 0.25 to 0.9 V (Ag/AgCl) at a scan rate 50 mV s⁻¹. The scan was repeated several times to ensure that a stable cyclic voltammetry (CV) was obtained. Voltammogram measurements for glycol oxidation were carried out in 0.5 M KOH+0.5 M glycol solution, and the potential was scanned from - 0.7 to 0.4 V (Ag/AgCl) at a scan rate 50 mV s⁻¹. Voltammogram measurements for glycerol oxidation were carried out in 0.5 M KOH+0.1 M glycol solution, and the potential was scanned from - 0.7 to 0.4 V (Ag/AgCl) at a scan rate 50 mV s⁻¹. Voltammogram measurements for methanol or ethanol oxidation were carried out in 0.5 M KOH +0.5 M methanol or ethanol solution, and the potential was scanned from - 0.9 to 0.6 V (Ag/AgCl) at a scan rate 50 mV s⁻¹.

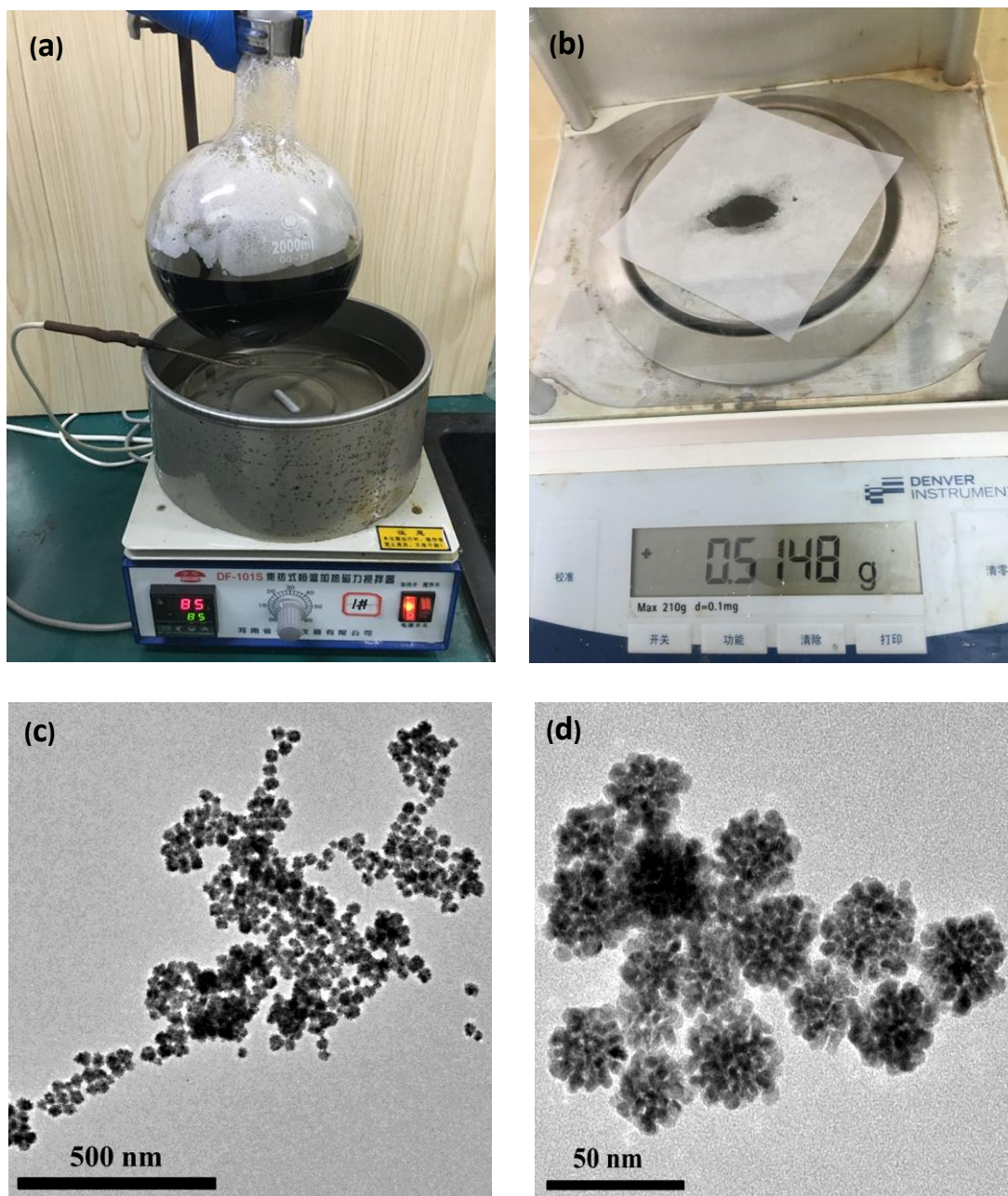


Fig. S1 (a, b) The digital photos of gram-scale synthesis of PdPt porous flowerlike nanoalloys with the Pt : Pd = 1:1. (c, d) The TEM images of the obtained product. (Note: Before weighing, the product were dried for overnight at 50 °C).

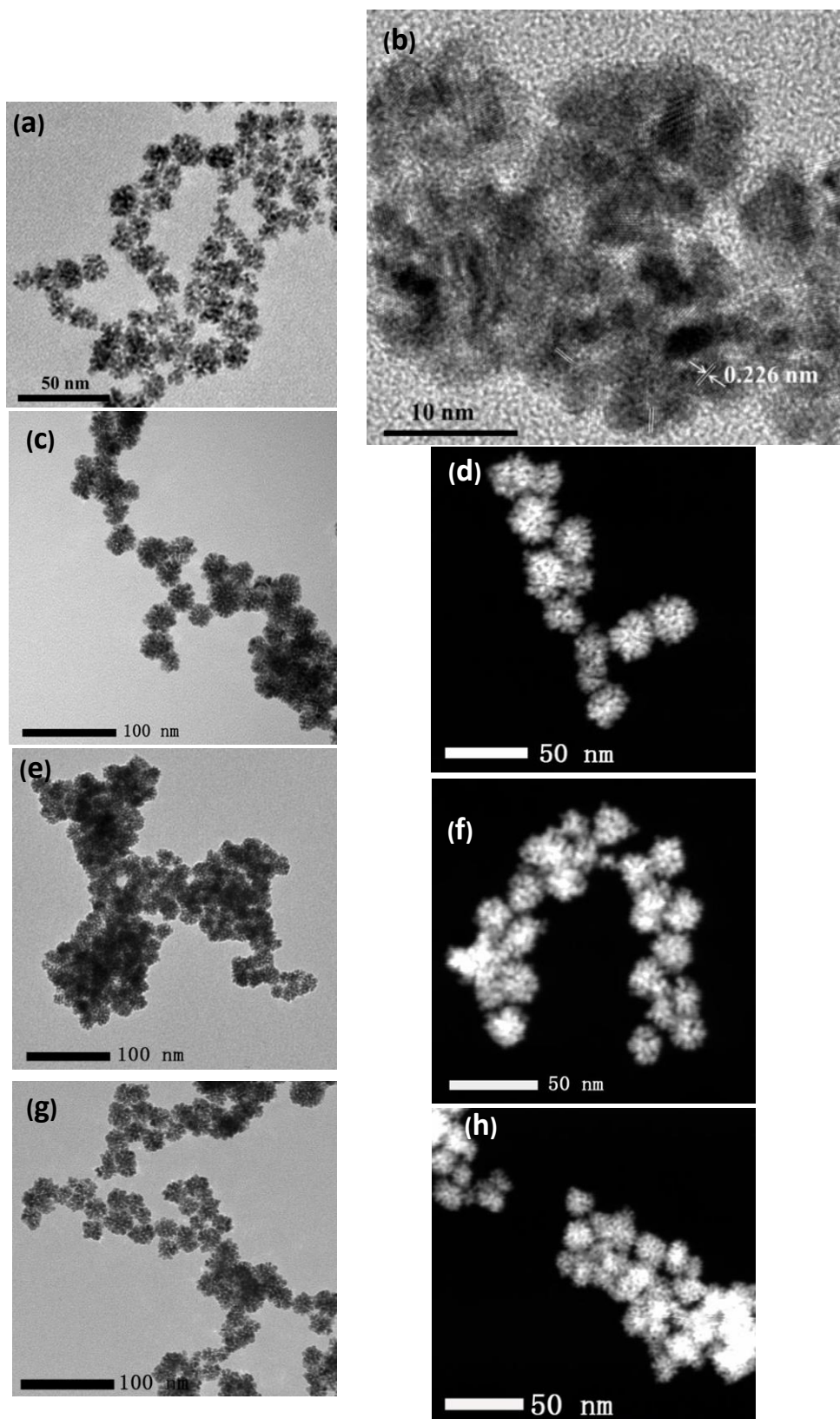


Fig. S2 TEM images of as-synthesized porous flowerlike pure Pt (a); Pd_{45.5}Pt_{54.5} (c); Rh_{3.1}Pt_{96.9} (e) and Rh_{3.4}Pd_{42.7}Pt_{53.9} (g) nanocrystals; (b) HRTEM image of flowerlike pure Pt; HADDF-STEM images of Pd_{45.5}Pt_{54.5} (d), Rh_{3.1}Pt_{96.9} (f) and Rh_{3.4}Pd_{42.7}Pt_{53.9} (h).

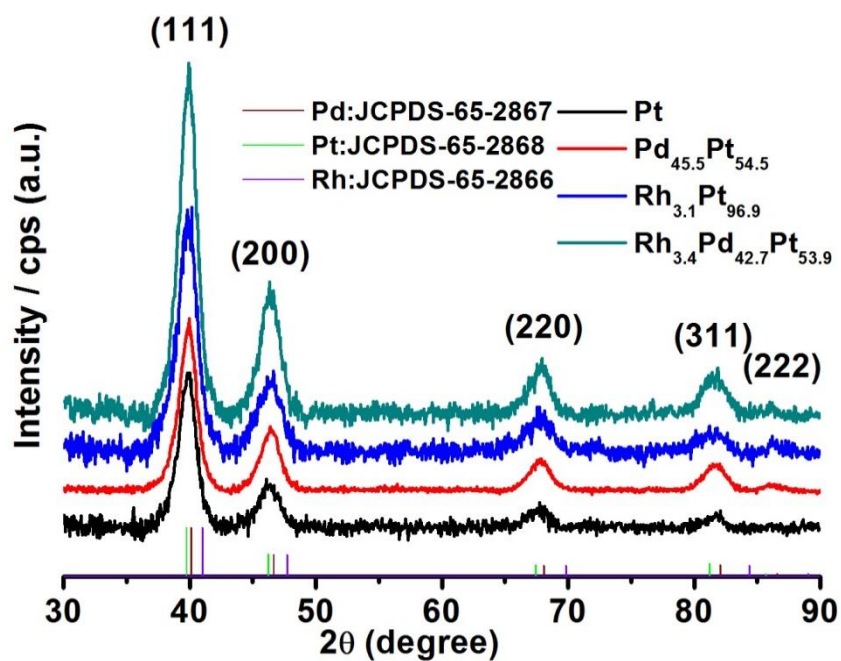


Fig. S3 XRD spectra of the as-synthesized flowerlike Pt, Pd_{45.5}Pt_{54.5}, Rh_{3.1}Pt_{96.9} and Rh_{3.4}Pd_{42.7}Pt_{53.9} nanocrystals. (The wine, the green and the violet lines in the XRD pattern stand for the standard peaks for Pd (JCPDS-65-2867), Pt (JCPDS-65-2868) and Rh (JCPDS-65-2866), respectively.)

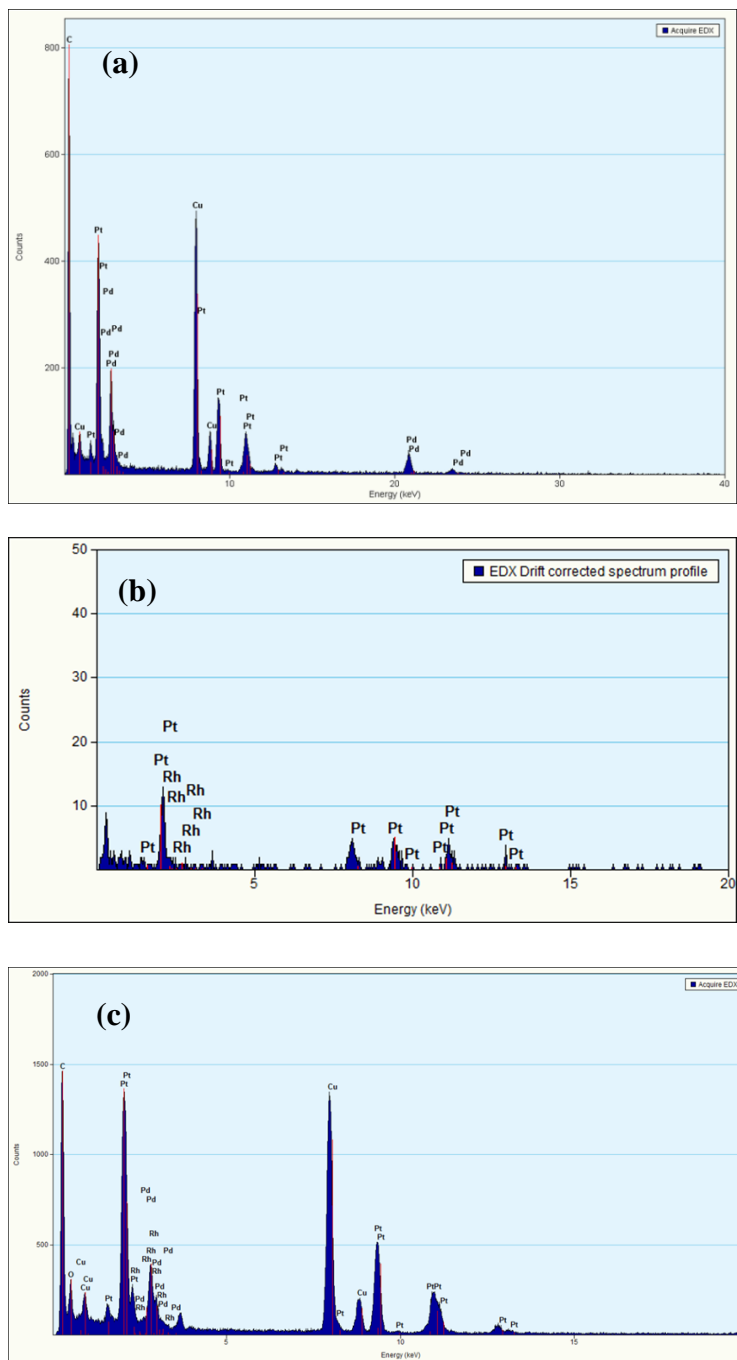


Fig. S4 EDX spectra of as-synthesized flowerlike Pd_{45.5}Pt_{54.5} (a), Rh_{3.1}Pt_{96.9} (b) and Rh_{3.4}Pd_{42.7}Pt_{53.9} (c) nanoalloys.

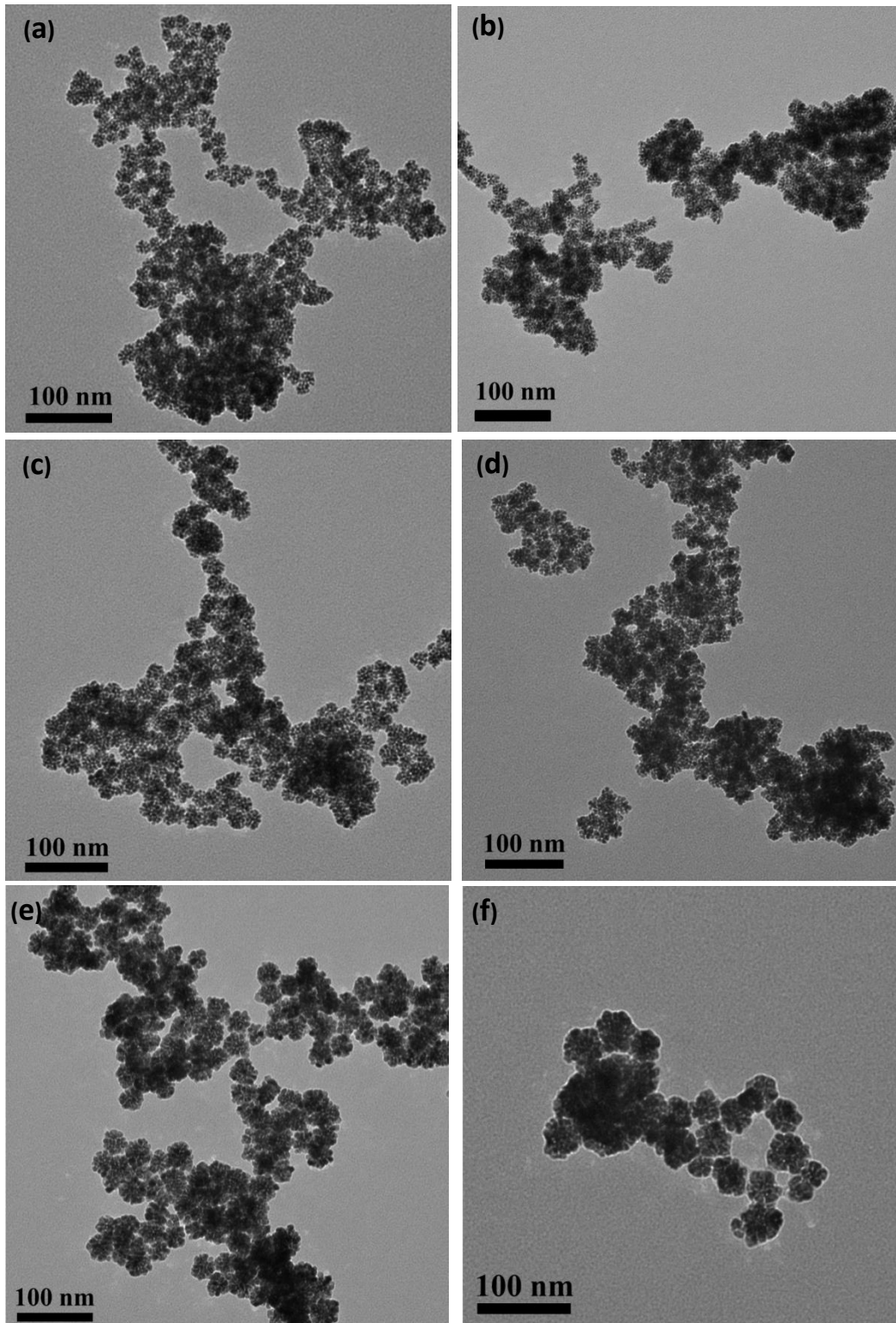


Fig. S5 TEM images of as-synthesized flowerlike PdPt nanoalloys with different Pt to Pd ratio. (a) 9:1; (b) 8:2; (c) 7:3; (d) 6:4; (e) 4:6 and (f) 3:7.

Sample	Element	Atom feeding ration	Atom%(results from ICP-MS)
Pd _{9.2} Pt _{90.8}	Pd	10	9.2
	Pt	90	90.8
Pd _{18.5} Pt _{81.5}	Pd	20	18.5
	Pt	80	81.5
Pd _{28.0} Pt _{72.0}	Pd	30	28.0
	Pt	70	72.0
Pd _{34.1} Pt _{65.9}	Pd	40	34.1
	Pt	60	65.9
Pd _{45.5} Pt _{54.4}	Pd	50	45.5
	Pt	50	54.5
Pd _{59.8} Pt _{40.2}	Pd	60	59.8
	Pt	40	40.2
Pd _{66.7} Pt _{33.3}	Pd	70	66.7
	Pt	30	33.3
Pd _{77.9} Pt _{22.1}	Pd	80	77.9
	Pt	20	22.1
Pd _{88.0} Pt _{12.0}	Pd	90	88.0
	Pt	10	12.0

Table S1. The composition of Pd and Pt of flowerlike nanocrystals calculated from ICP-MS.

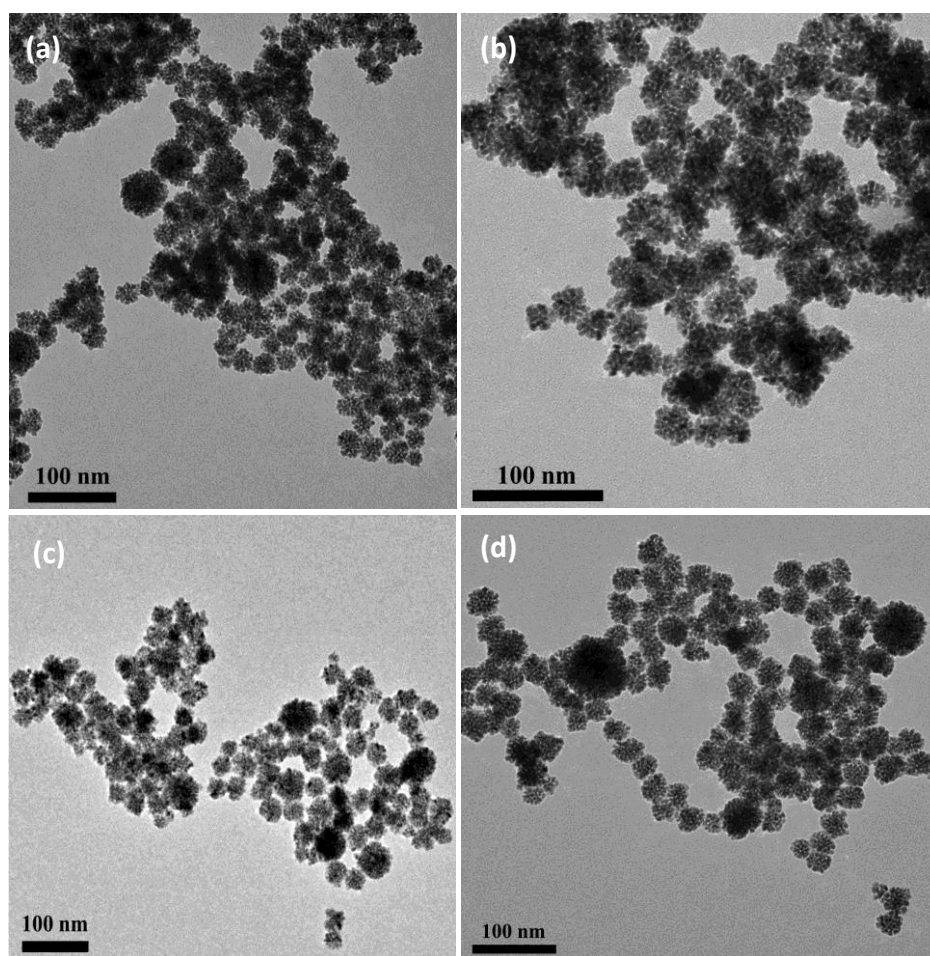


Fig. S6 TEM images of as-synthesized flowerlike RhPdPt nanoalloys. (a) $\text{Rh}_{1.9}\text{Pd}_{29.0}\text{Pt}_{69.1}$; (b) $\text{Rh}_{3.4}\text{Pd}_{42.7}\text{Pt}_{53.4}$; (c) $\text{Rh}_{2.1}\text{Pd}_{50.3}\text{Pt}_{47.6}$ and (d) $\text{Rh}_{2.7}\text{Pd}_{61.6}\text{Pt}_{35.7}$

Sample	Element	Atom feeding ration	Atom%(results from ICP-MS)
$\text{Rh}_{1.9}\text{Pd}_{29.0}\text{Pt}_{69.1}$	Rh	10	1.9
	Pd	30	29.0
	Pt	60	69.1
$\text{Rh}_{3.4}\text{Pd}_{42.7}\text{Pt}_{53.4}$	Rh	10	3.4
	Pd	40	42.7
	Pt	50	53.4
$\text{Rh}_{2.1}\text{Pd}_{50.3}\text{Pt}_{47.6}$	Rh	10	2.1
	Pd	50	50.3
	Pt	40	47.6
$\text{Rh}_{2.7}\text{Pd}_{61.6}\text{Pt}_{35.7}$	Rh	10	2.7
	Pd	60	61.6
	Pt	30	35.7

Table S2 The composition of porous flowerlike RhPdPt nanocrystals calculated from ICP-MS.

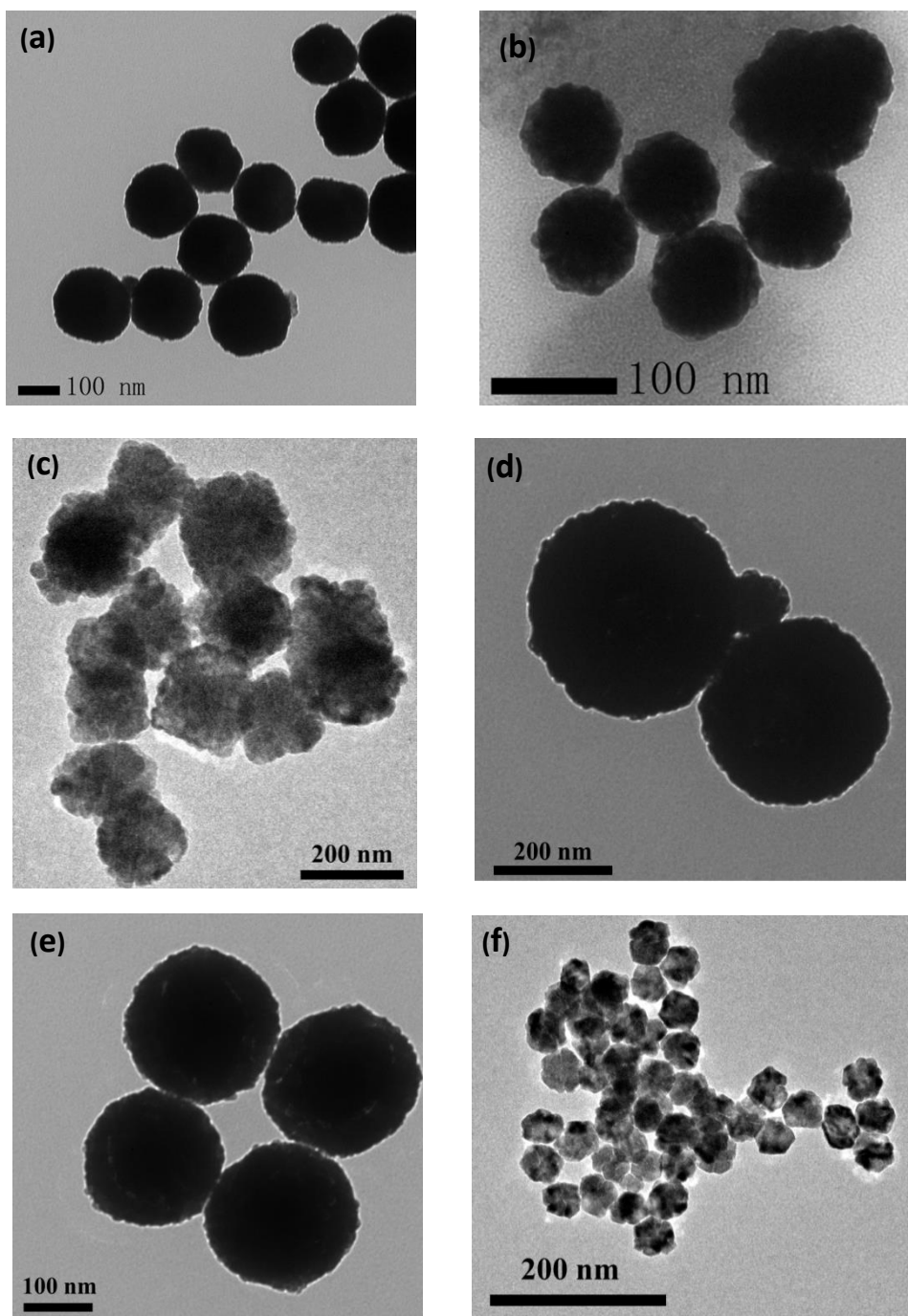


Fig. S7 TEM images of as-synthesized product (a) without glycine; (b) without CTAC; (c) only using Pd precursors; (d) the Pd to Pt precursor ratio was 8 : 2; (e) the Pd to Pt precursor ratio was 9 : 1 and (f) without using H_2PtCl_6 , only using Rh and Pd precursors.

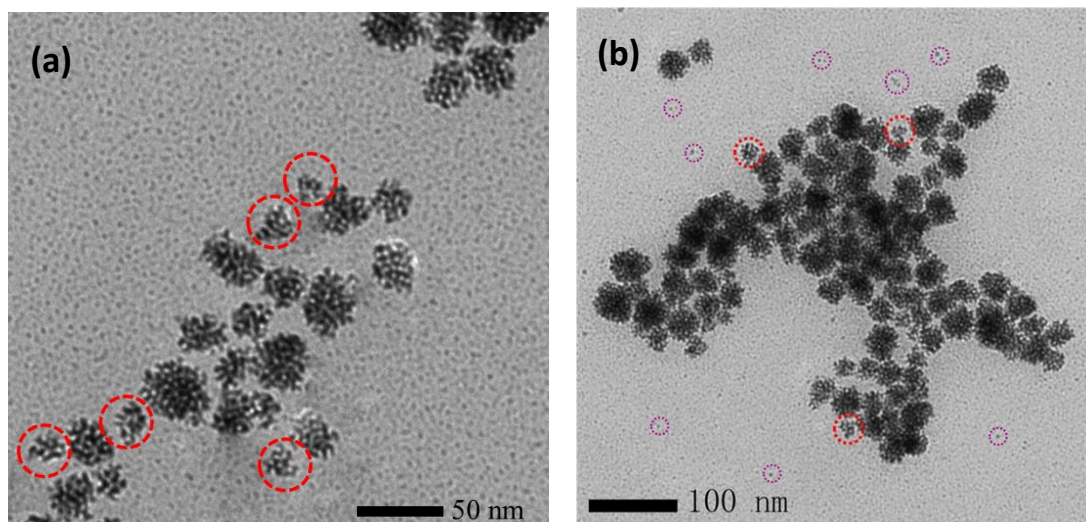


Fig. S8 TEM image of the as-synthesized product obtained for 20(a) and 30(b) minutes. (There are a large number of small particles in Fig. S8a. Intense purple circle: single primary spherical nanocrystals; red circle: primary flowerlike nanocrystals)

Catalysts	ECSA		Methanol oxidation		Glycerol oxidation		Ethanol oxidation		Glycol oxidation	
	$\text{m}^2\text{g}^{-1}\text{Pt}$	$\text{m}^2\text{g}^{-1}\text{metal}$	Mass activity (A mg^{-1}Pt)	Mass activity (A $\text{mg}^{-1}\text{metal}$)	Mass activity (A mg^{-1}Pt)	Mass activity (A $\text{mg}^{-1}\text{metal}$)	Mass activity (A mg^{-1}Pt)	Mass activity (A $\text{mg}^{-1}\text{metal}$)	Mass activity (A mg^{-1}Pt)	Mass activity (A $\text{mg}^{-1}\text{metal}$)
Pt	72		2.83		2.88		3.59		7.82	
$\text{Pd}_{45.5}\text{Pt}_{54.5}$	74	51	5.26	3.63	3.00	2.06	6.97	4.80	8.58	5.86
$\text{Rh}_{3.1}\text{Pt}_{96.9}$	21	20.9	0.80	0.79	0.86	0.85	1.11	1.10	3.62	3.61
$\text{Rh}_{3.4}\text{Pd}_{42.7}\text{Pt}_{53.9}$	48	33	3.35	2.29	2.83	1.95	4.15	2.85	6.08	4.18
Pt black	21		1.43		0.81		1.51		1.84	

Table S3. Comparison of the electrocatalytic properties of flowerlike Pt-based nanocrystals and the commercial Pt black.

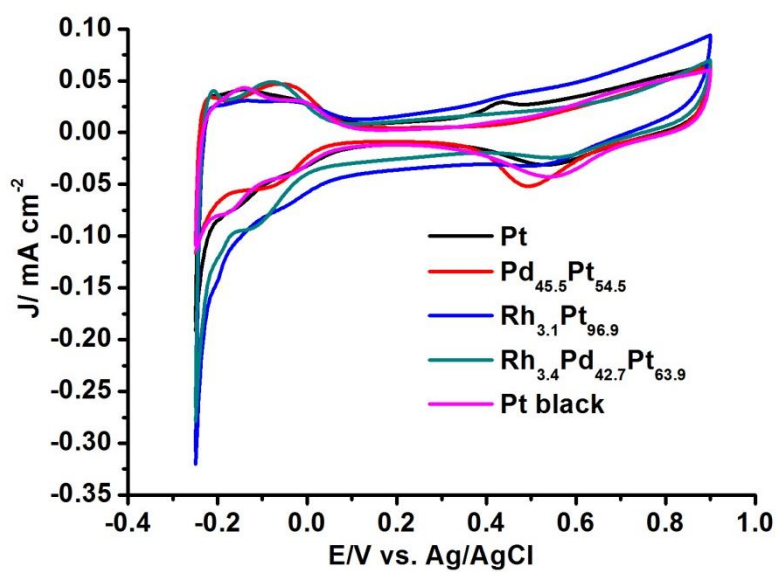


Fig. S9 CVs of the as-synthesized flowerlike pure Pt, Pd_{45.5}Pt_{54.5}, Rh_{3.1}Pt_{96.9}, Rh_{3.4}Pd_{42.7}Pt_{53.9} nanocrystals and the commercial Pt black in a 0.1 M HClO₄ solution with a scan rate of 50 mV/s. The hydrogen adsorption/desorption method was used to measure the ECSA (m²g⁻¹) of these catalysts.

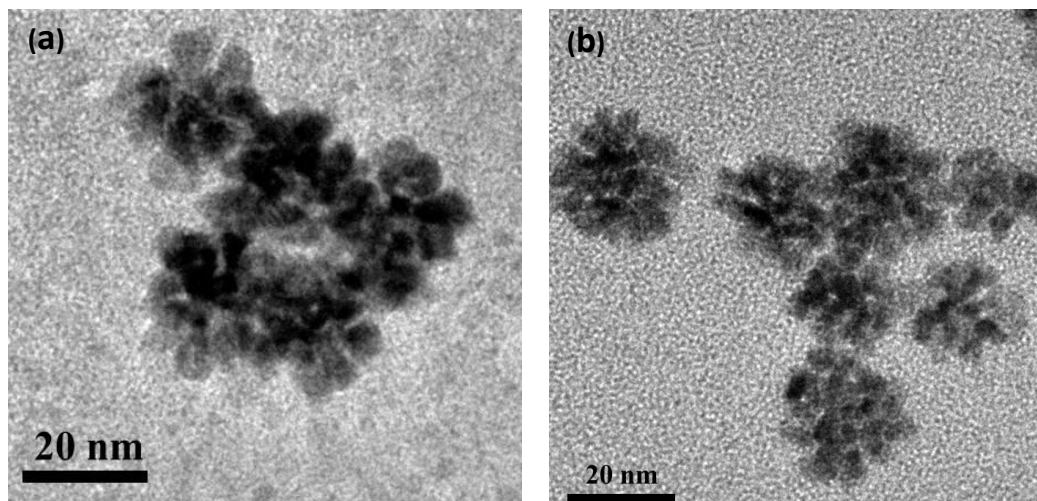


Fig. S10 The TEM images of porous flowerlike Pd_{45.5}Pt_{54.5} after current-time test (a) and accelerated durability test (b).